Peer-reviewed version available at Materials 2020, 13, 2519; doi:10.3390/ma13112519

Collapse Mechanism of Single-Layer Cylindrical Latticed Shell Under Severe Earthquake

Haitao Zhou[1,2]; Yigang Zhang[2];Feng Fu[3]; Jinzhi Wu[2]

[1,]*Henan University of Urban Construction, Henan,467001, China*
Email :Chinaazhouhaitao111111@163.com
[2]*Professor, Spatial Structure Research Center, Beijing University of Technology, Beijing,100124, China and Key Lab of Urban Security and disaster Engineering, MOE, Beijing University of Technology, Beijing,100124, China. Email: bzyg@bjut.edu.cn, kongjian@bjut.edu.cn*
[3] *Corresponding Author, Lecturer, School of Mathematics, Computer Science & Engineering, Department of Civil Engineering, Northampton Square, London, C1V 0HB,U.K. feng.fu.1@city.ac.uk*

Abstract

In this paper, the results of finite element analyses of a single-layer cylindrical latticed shell under severe earthquake is presented. A 3D Finite Element model using fiber beam elements were used to investigate the collapse mechanism of this type of shell. The failure criteria of structural members are simulated based on the theory of damage accumulation. Severe earthquake of peak ground acceleration (PGA) of 500 gal was applied to the shell. The stress and defeomation of the shell were studied in detail. A three-stages collapse mechanism “double-diagonal -members-failure-belt” of this type of structure was discovered. Based on the analysis results, the measures to mitigate collapse of this type of structure is recomanded.

Keywords Cylindrical latticed shell, damage accumulation, progressive Collapse, Finite Element,Earthquake

1. Introduction

After the events of September 11, 2001, more and more researchers have carried out research work on investigation of the mechanism of progressive collapse in buildings, trying to find possible mitigating methods. But few studies have been performed for space structures. As a typical long-span space structure, single-layer cylindrical

Peer-reviewed version available at Materials 2020, 13, 2519; doi:10.3390/ma13112519

reticulated dooms are widely used in public buildings, such as terminals, gymnasiums, large factories and so on for its graceful appearance. However, if the dome collapses under severe earthquake, heavy casualties and economical losses would be caused. Therefore, research in this area is imperative.

In the current design practice, some design procedures are available in Europe and the United States on mitigating the progressive collapse of buildings，such as the design guidance of the Department of the American Concrete Institute (ACI) [1] and the General Services Administration (GSA) [2] in which specific process of assessment on the necessity of anti-collapse design is recommanded. In the American Society of Civil Engineers (ASCE) [3] ductility and sufficient connection performance of the structure is required. In Eurocode 1 [4], it is stipulated that the structure must be able to resist a certain accidental load without a large scale of collapse. Those specifications aimed at mitigating of the collapse of structures under specific accidents. In Eurocode 2 [5], special requirements are given to the construction of reinforced concrete, especially about the anchorage and connection of bars. Some references such as FEMA [6] and NIST [7] also provide general design recommendations, which require steel-framed structural systems to have enough redundancy and resilience. However, most of these design codes focused on buildings, no detailed design procedure to prevent progressive collapse of reticulated shells is available.

Up to now, some numerical investigations and experimental tests have been carried out on building structures. In 1974 Mc Guire [8] reviewed the problem of progressive collapse of multi-story masonry buildings under abnormal loading and presented some recommendations to prevent progressive collapse. Shimada [9] conducted a shaking table test of a full-scale 2-story and 1×1 span steel frame model in 2007. Song [10] conducted a test on a steel frame building by physically sudden removal of four

Peer-reviewed version available at *Materials* **2020**, *13*, 2519; doi:10.3390/ma13112519

columns at ground level to investigate the load redistribution within the building. Chen, J.L [11] conducted a progressive collapse resistance experiment on a two-storey steel frame in which composite concrete slab was adopted. Tsitos, [12] performed a quasi-static “push-down” experiments on a 1:3 scale three-story steel frame considering multi-hazard extreme loading. Starossek [13] suggested a pragmatic approach for designing against progressive collapse and a set of design criteria. Lim, [14] investigated progressive collapse of 2D steel-framed structures with different connection and found that horizontal column buckling propagation control was the only solution. Yamazaki [15] clarified the frame conditions which enable stories to resist progressive collapse through comparing the gravity potential energy released by the story collapse with the energy which columns absorbe before they completely collapse due to the compressive load. O'Dwyer [16] presented details of an algorithm for modelling the progressive collapse of framed multi-story buildings.

However, as it can be seen that, most of above research is related to building structures; little has been carried out on long-span space structures. Zheng et al.[17] developed a force–displacement hysteresis model for the collapse simulation of a power transmission pylon considering the buckling/softening-based fracture criterion. Rashidyan et al.[18] recomended the method of strengthening the compression layer members along with weakening the tension layer members of double-layer space trussesis was an effective method for increasing the structure’s ductility and load-bearing capacity against progressive collapse. To study the progressive collapse phenomenon of structures during earthquakes, Lau et al.[19] carried out an nonlinear analyses of reinforced concrete bridges by the Applied Element Method (AEM). Miyachi et al.[20] carried out a progressive collapse analysis for three continuous steel truss bridge models with a total length of 230.0 m using large deformation and elastic

plastic analysis. Takeuchi et al.[21] proposeed the post-fracture analysis methods for truss structures composed with tubular members of large diameter-to-thickness ratios, and investigated the collapse mechanism of such truss towers after the buckling and fracture of main columns and diagonals. Ponter et al.[22] discussd of the programming method based on the Elastic Compensation method used for limit and shakedown analysis of steel structures. Skordeli et al.[23] studied examples of limit and push down analysis of spatial frames under the aforementioned ellipsoidal approximations with several aspects discussed. Starting from a computational formulation for the elastoplastic limit analysis of 3D truss-frame systems, apt to provide the exact limit load multiplier and attached collapse mechanism. Ferrari et al.[24] derived a full evolutive piece-wise-linear response of the bridge, for different try-out loading configurations. Xia et al.[25] studied the dynamic behavior of snap-through buckling in single-layer reticulated domes, based on the nonlinear equilibrium equations. Kato et al. [26] peformed an analysis on buckling collapse and its analytical method of steel reticulated domes with semi-rigid ball joints, on the basis of a nonlinear elastic-plastic hinge analysis formulated for three-dimensional beam-columns with elastic perfectly plastic hinges located at both ends and the mid-span for each member.

However, those researches focused on the response of the space structure under static load, little research has been done for the collapse mechanism of a space structure under seismic load. Under seismic load, damage accumulation induced by cyclic loading is a very important factor that needs to be considered for its effect on the numerical simulation of the deterioration of both the stiffenss of the dome and strength of materials, and the fracture of members. In another word, an accurate prediction of the dynamical response of structures needs serious attention to be paid on damage

accumulation. However, in most of the numerical models used in above research, damage accumulation is ignored, little work has been done in this area. In this paper, based on thermodynamic theory, the damage evolution equations for fiber beam elements derived by the authors [27] is used to simulate the progressive collapse mechanism of single-layer cylindrical latticed shell. The corresponding constitutive relationship for beam elements and the relevant numerical analysis method are also developed.

Due to the redundancy and indeterminacy of single layer space structures, a dynamic instability criterion based on an implicit algorithm can capture neither the collapse mechanism of the reticulated shell nor the failure mode of individual components. Therefore, the simulation of the whole collapse process requires application of an explicit dynamic algorithm, which is used in this paper. Based on the above studies, in Zhou et al.[27], the authors developed a subroutine program based on an explicit dynamic algorithm to analyze the response of the single-layer reticulated shell under a severe earthquake. The program was validated against experimental tests. It is proved that the proposed numerical method can accurately simulate the members' failure, the redistribution of internal forces, and the collapse mechanism of the whole structure. Based on this numerical method, parametric studies on single-layer reticulated shell are performed and the collapse mechanism of this type of structure is studied.

2. The Numerical model

The collapse analysis is performed by general purpose program ABAQUS through the further development of the subroutine VUMAT program in Abaqus. The numerical method introduced in Zhou et al. [27] is used in this research. All the structural members of the reticulated shell are simulated using the beam elements. Each beam element is further discretized into eight longitudinal fibers across their cross-section

Peer-reviewed version available at Materials 2020, 13, 2519; doi:10.3390/ma13112519

with appropriate constitutive model defined to each fiber as is shown in Fig 2.

In the dynamic analysis, below damage critrien is used:

$$dD = \frac{1-D}{2\sigma_{11}} d\sigma_{11} \tag{1}$$

Where,

σ_{11} is normal stress existing in a beam element,

D is cumulative damage

The failure criterion of each fiber is determined based on the studies by the authors in (2018). When D_{new} in a fiber develops into certain value D_{limt}, the fiber is determined as failure. D_{limt} is determined using below formula:

$$D_{\text{limt}} = 1 - \left(\frac{f_u}{f_y} \right)^{-\frac{1}{2}}$$

In the designed VUMAT subroutine program, when the failure of one fiber is triggered, the elastic modulus of this fiber will be set as zero. When all the fibers in a beam element fail, that beam element is determined as failure, thus this beam element will be deleted by the program. Therefore, the process of collapse of the dome can be simulated. After an element is deleted due to failure, the explicit dynamic analysis based on Central difference method, which enabling the accurate capture of the response of the dome. For detailed explanation of the numerical algorithm, please refer to Zhou et al.[27].

3. Progressive collapse analysis of single-layer cylindrical latticed shell

Base on afrometioned analysis method, a single-layer monoclinic cylindrical reticulated dome with span of 20m, 30 metres in length and 7.5 metres in height was modeled using general purpose program Abaqus (Fig. 1). The dome was pin supported

along the two longitudinal edges. All the structural members are Chinese steel tubular sections, where, the lateral and diagonal diagonal members member are Chinese Ø166 × 5, and the longitudinal member are Chinese Ø114 × 5. The grade of the steel was Chinese Q235-B, with an initial yield stress of 235 MPa. The Young's modulus is 2.06 × 10^5 MPa. The Poisson ratio was 0.3. The live load of the roof was taken as 2.5 KN/m^2. Figure 1 also shows the structural zone divided by the authers, which is to clearly demonstate the response of the dome under earthquake loading.

In the simulation, all the structural members were modeled using beam elements. Each beam element was divided into four segments along its length to model the buckling behavior. as it is explained Zhou et al. [27], this is an effective way to model the member buckling with sufficient accuracy. In addition, each beam element was subdivided into eight fiber beams across its cross-section as shown in Fig.2. The fibers are numbered from 1 to 8 accordinly along the circumference of the beam element (Fig.2).

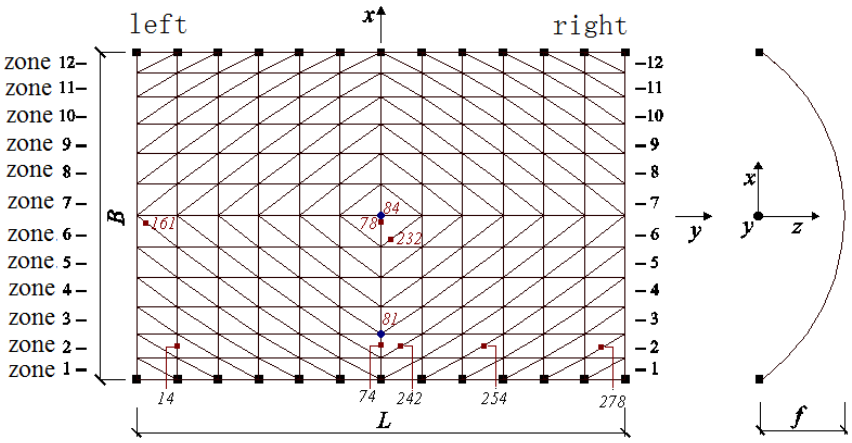

a structural zone in the model

Preprints (www.preprints.org) | NOT PEER-REVIEWED | Posted: 2 May 2020 doi:10.20944/preprints202005.0012.v1

Peer-reviewed version available at Materials 2020, 13, 2519; doi:10.3390/ma13112519

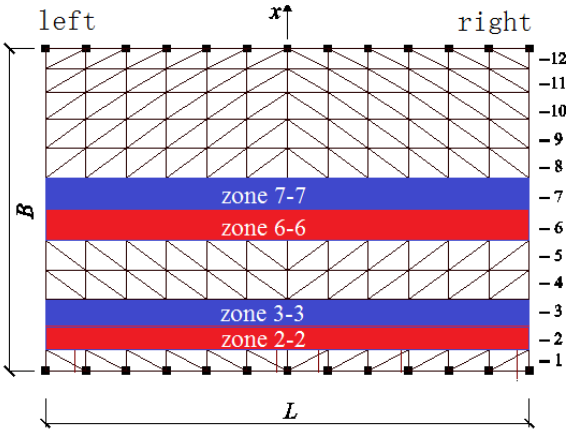

b structural zone in the dome

Figure 1 Single-layer cylindrical latticed shell with structural zone denotaed

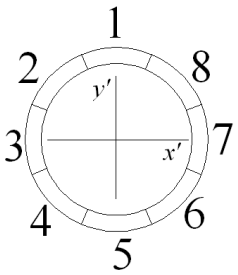

Figure 2 The location and numbering of the fibers in a signle beam element

The analysis was divided into two steps. The first step was static analysis, where the gravity load was applied to the dome. The second step was dynamic analysis, where the time history of the Taft earthquake was applied at the support, in X, Y, and Z directions, with the peak ground acceleration (PGA) of 500 gal in the X direction, 0.85 times 500 gal in the Y direction, and 0.65 times 500 gal in the Z direction, respectively. The time duration was 20s, which is greater than 10 times the natural period of the dome. The constitutive model of the material is using the hybrid hardening model and the modulus considered the cumulative effect of damage to simulate the performance deterioration of material occured during plastic tension in hysteresis process under seismic loading.

Fig. 3 depicts deformation and damage distribution during the collapse process, where the distribution of the D value can be checked. It demonstrates the process where the D

Preprints (www.preprints.org) | NOT PEER-REVIEWED | Posted: 2 May 2020 doi:10.20944/preprints202005.0012.v1

Peer-reviewed version available at Materials 2020, 13, 2519; doi:10.3390/ma13112519

value was zero, which indicate no danage was developed until the rupture of the member when $D>D_{limt}$

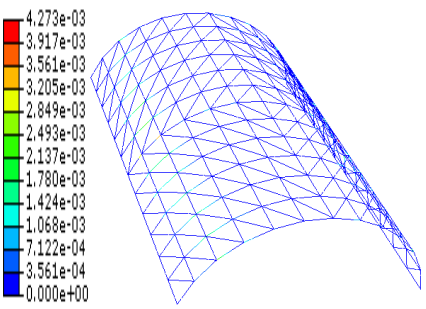

a t=4.56s

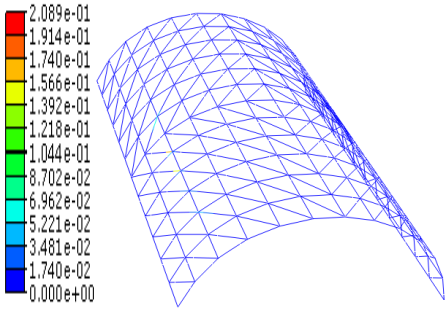

b. t=6.16s

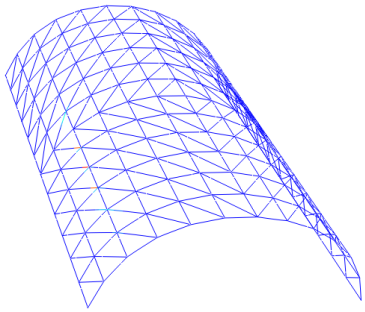

c. t=11.78s

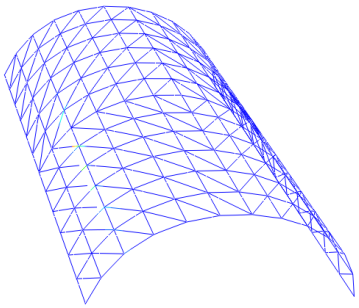

d. t=11.80s

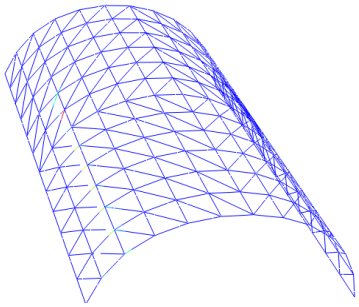

e. t=12.03s

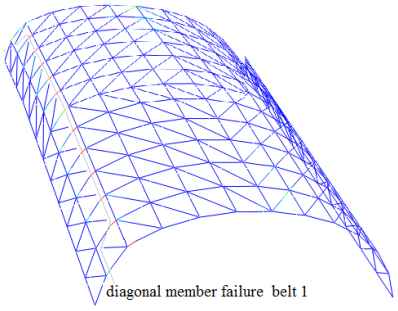

f. t=14.38

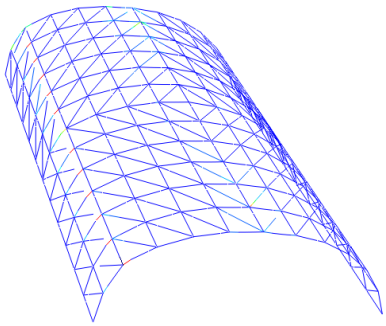

g. t=15.40s

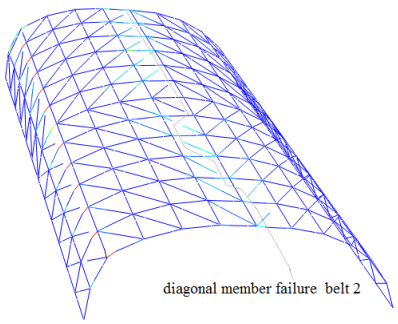

h. t=15.83s

Preprints (www.preprints.org) | NOT PEER-REVIEWED | Posted: 2 May 2020 doi:10.20944/preprints202005.0012.v1

Peer-reviewed version available at Materials 2020, 13, 2519; doi:10.3390/ma13112519

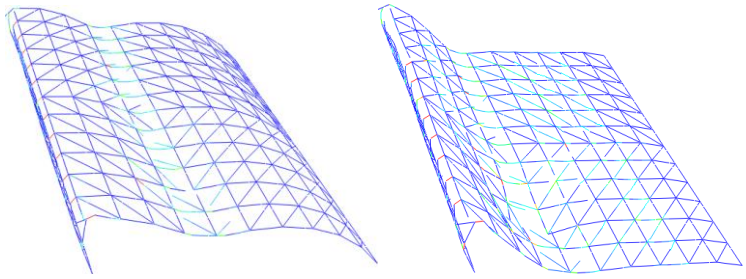

i. t=16.38s j. t=16.78s

Figure 3 deformation and damage distribution of structural members during the collapse process

According to the analysis results, the dome entered into plastic stage at 1.88s for the first time. Damage distribution spread to zone 2-2 and 3-3 and symmetric zone of 6-6/7-7, but D value was extremely small in this stage. With the ground motion continued, at 6.16s, D value of many diagonal and lateral members in the . zones of 2-2 and 3-3, at djacent ends, had obviously exceeded that of members in other zones(Fig.3 b). Untill 11.78s, the damage state of whole dome had furtherly deteriered . The D value of damaged structural members keeped rising and more diagonal and lateral members were damaged. At 11.80s, 3 diagonal bars in zone of 2-2 failed at ends of the joints with a threshold value 0.209.

At 12.03s, all the diagonal members in the zone 2-2 failed, while the damage range spread to the left of the zone, with the damage area increased dramatically , although no member facture was observed. At 14.38s, all the diagonal members in the zone 2-2 failed because of continous damage accumulation, and the failed zone was like a continuous and regular “diagonal member failure belt”. Lateral bars were left unbroken , damage area continue to propogate. The deflection of dome had been significant . And some lateral members and diagonal members in the zone 6-6/7-7 were damaged already.

Afterword, damage area was in between the zone of 6-6/7-7. At 15.40s, most diagonal members in the zone were damaged and a few at two longitudinal ends

Preprints (www.preprints.org) | NOT PEER-REVIEWED | Posted: 2 May 2020 doi:10.20944/preprints202005.0012.v1

Peer-reviewed version available at Materials 2020, 13, 2519; doi:10.3390/ma13112519

failedd. Untill 15.83s, most diagonal members in the zone of 6-6 and two diagonal members at the right of zone of 7-7 failed. The position of structural members failed in a similar manner of "diagonal member failure belt"silghtly wider than the first came into being(Fig.3h). No

Lateral members failed though with obviously damaged. And the overall downward deflection of the dome become significant during this process. With the continuous action of earthquake, the dome begins to collapse downward rapidly. Horizontally the dome collapsed towards the position of first "diagonal member failure belt", the whole dome now looked like a italic letter "M". Finally, 1.13s later the forming of the second "diagonal member failure belt", the dome collapsed totally. The D value of longitudinal bars of the dome had not increased much throughout.

3.1 Collapse pattern of "Double-diagonal member failure belt"

Fig. 4 depicts deformation and distribution of the damage of the structural member during the collapse process for the other two domes, with a span:depth ratio of 4:1 and 2:1 repsectively. Their span are kepted as 20-m-span. Fig. 5 depicts that of the other two 20-m-span domes, one with a length: width ratio of 1:1, another 1:2. With the increase of length: width ratio, the position of the two "diagonal member failure belt" moved from the zone of 2-2/6-6 to 3-3/7-7. The decrease of length: width ratio caused contrary trend. Besides of above, the basic process of collapse and final collapse form are similar.

Fig.6 depicts the failure mode of double-diagonal member cylindrical reticulated dome are similar to single- diagonal member cylindrical reticulated dome.

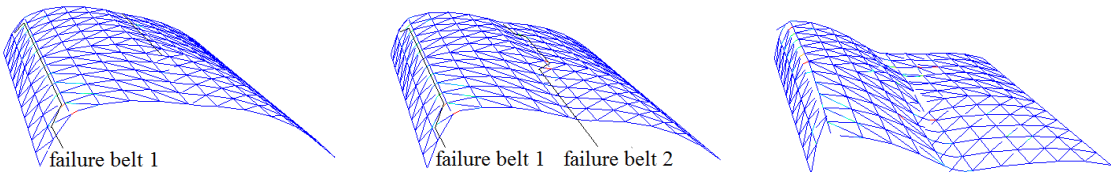

a1 belt 1 formed a2 belt 2 formed a3 dome collapses

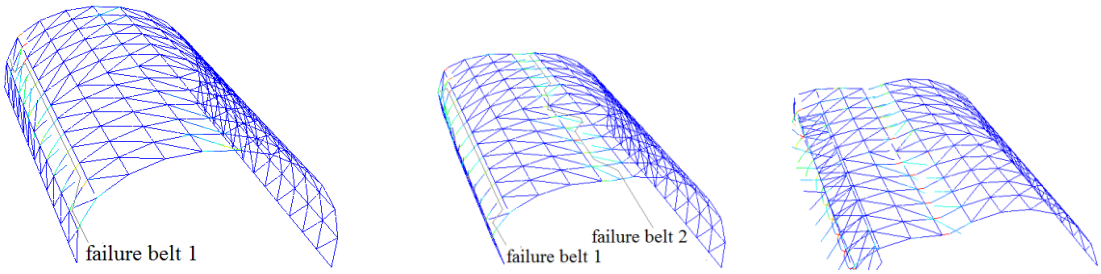

b1 belt 1 formed b2 belt 2 formed b3 dome collapses

Fig 4 collaps process of cylindrical reticulated dome of diffrerernt span: depth ratios at typical times (a span/depth=4:1, b span/depth=2:1)

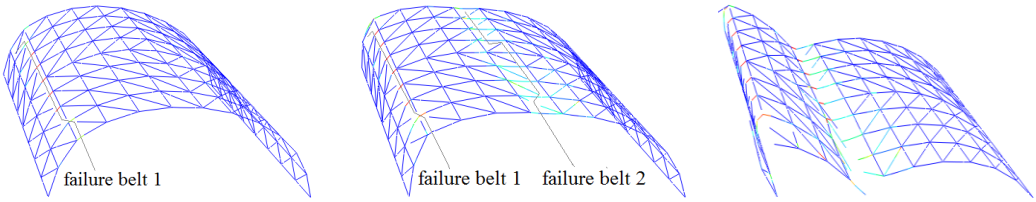

a1 belt 1 formed a2 belt 2 formed a3 dome collapses

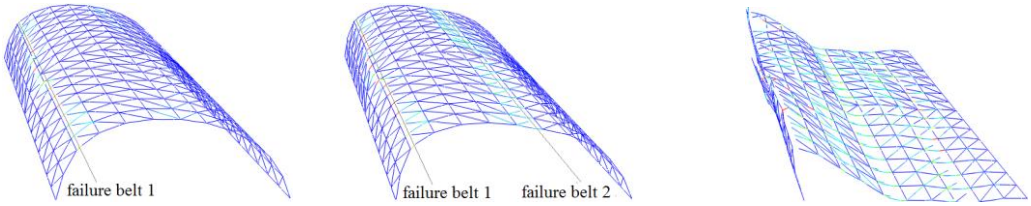

b1 belt 1 formed b2 belt 2 formed b3 dome collapses

Fig 5 collaps process of cylindrical reticulated dome of different length: width ratios at typical times (a length/depth=1:1, b length/depth=2:1)

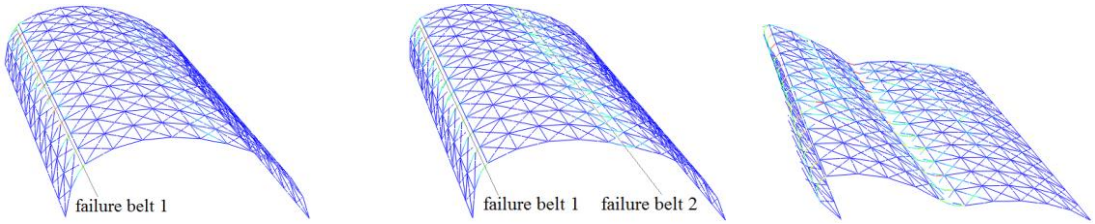

a1 belt 1 formed a2 belt 2 formed a3 dome collapses

Figure 6 Double diagonal member failure belt

Apart from above analysis, extensive parametric studies were performed by the authors with diferent spans, diferent span:depth ratios, diferent length: width ratios, diferent roof loadings. It has proved that the similar collapse process were observed.

In addition to above case studies, all the analysis cases was applied with the peak

Preprints (www.preprints.org) | NOT PEER-REVIEWED | Posted: 2 May 2020 doi:10.20944/preprints202005.0012.v1

Peer-reviewed version available at Materials 2020, 13, 2519; doi:10.3390/ma13112519

ground acceleration (PGA) of 500 gal in the Y direction, 0.85 times 500 gal in the X direction, which is different to the first loading regime. The results showed that nothing but the time when dome collapsed changed.

Therefore, a consistent failure pattern for the collapse process of single-layer cylindrical reticulated domes can be concluded. Under severe earthquake, seriously damaged first occurs at 1/4 height of the dome. Diagonal members failed continuously from nearly center to boundary along the lengthwise and the first “diagonal member failure belt” come into being(Fig.7). The stiffness of dome is also greatly weakened. Then another damaged zone appear at middle of dome and in the zone diagonal members failed continuously from ends to nearly center along the lengthwise. A second “diagonal member failure belt” was formed. The stiffness of dome is reduced further. The whole deflection become significant. The position of two “belt” varied slightly with the change of geometry. At final stage, the dome deflect rapidly at the second “belt”, with dropping twords the first “belt”. The dome collapse. The paper calls the collapse process and phenomen as “double-diagonal -members-failure-belt” pattern.

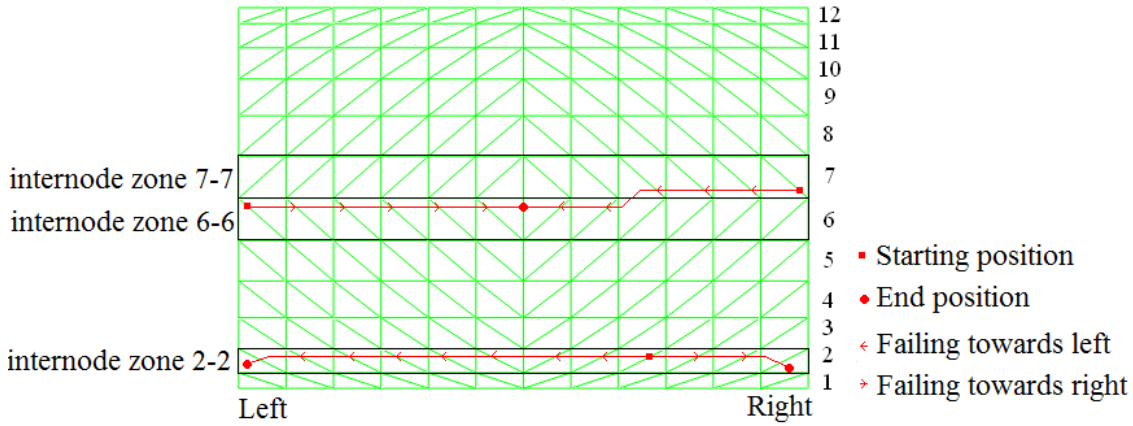

Figure 7 the demonstration of the collapse mechnism of the shell

3.2 Mechanism of progressive collapse process

Earthquake loading cause deformation and material damage. Deformation and damage cause variety of mechanical characteristics of dome. The variety deeply affect the deformation and development of material damage in turn ("failure" is the extreme state). This kind of complex relationship exists and works during the whole process.

According to the analysis results in the earlier section, it can be concluded that, of the deformation and mechanical characteristics of dome changed along the whole process, diferent of deformation characteristics and mechanism properties were observed, the collapse process can be divided into three stages.

Stage 1: this stage refers to process from earthquake occuring to the formation of the first "belt" (0-14.38s). during this stage the phenomenon of material damage and diagonal members failing mainly occur in the zone of 2-2.

The cylindrical reticulated dome, with longitudinal edges pin suppoted, is one type space structure exihibit planary arch features . The response of dome under severe earthquake is very simlary to that of a palne arch. The diagonal members works as the bracing, and the longitudinal member works as tie bar which coordinates the continuity of the vertical and horizontal deformation, Therefore, during earthquake, axial force, bending moment and torsion of each kind of bars vary with time, although, overall characteristics are relatively stable.

So at the beginning of earthquake, the maxium internal force can be observed at 1/4 span of dome from the boundary, and the member that first developed into plastic state caused material damage must come from this zone. This had been proved in the paper (Figure 3a)

Preprints (www.preprints.org) | NOT PEER-REVIEWED | Posted: 2 May 2020 doi:10.20944/preprints202005.0012.v1

Peer-reviewed version available at Materials 2020, 13, 2519; doi:10.3390/ma13112519

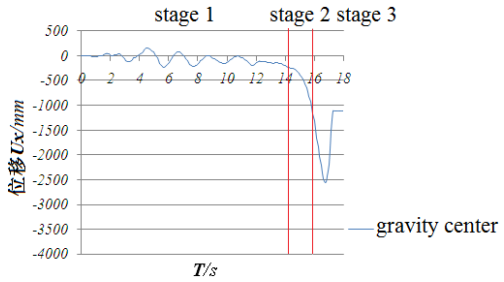

Figure 8 The gravity center of the structure

However, Earthquake loading is asymmetric, so plastic deformation and damage accumulation on dome is inevitablly asymmetric. This means D value and increasing speed of D value of bars in this zone is larger than those of bars in other zones. With the continuing of ground motion and gradual increasing of amplitude, 5.13s later, gravity center of dome moved towords x direction obviously (Figure 8). This is because plastic deformation occured in vibration, and the overall geometric configuration shifted towards zone of 2-2. This phenomenon conversly caused that internal forces of member in zone of 2-2/3-3 were significantly larger that in symmetric zone of 11-11/10-10. Consquenly, the development speed of damage of bars in zone of 2-2 were more than that of bars in the symmetric zone(Fig.3b and 3c).

As it shown in Figure 9,Through the comparison of the time history curves of bending moment $M_{x'}$and $M_{y'}$, torsion $M_{x'y'}$and axial force F of members 242/254/278 in zone of 2-2, it can be found that although the axial force F of 254 was less than that of 242, bending moment $M_{x'}$and M_y, torsion $M_{x'y'}$ of 254 is obviously larger than those of 242. Axial force and bending moment of 278 are approximate to those of 254, but torsion of 278 is less than that of 242. So D values of slant bar 254 and neighbouring bars in zone of 2-2 are obviously larger than those of other bars.

Preprints (www.preprints.org) | NOT PEER-REVIEWED | Posted: 2 May 2020 doi:10.20944/preprints202005.0012.v1

Peer-reviewed version available at Materials 2020, 13, 2519; doi:10.3390/ma13112519

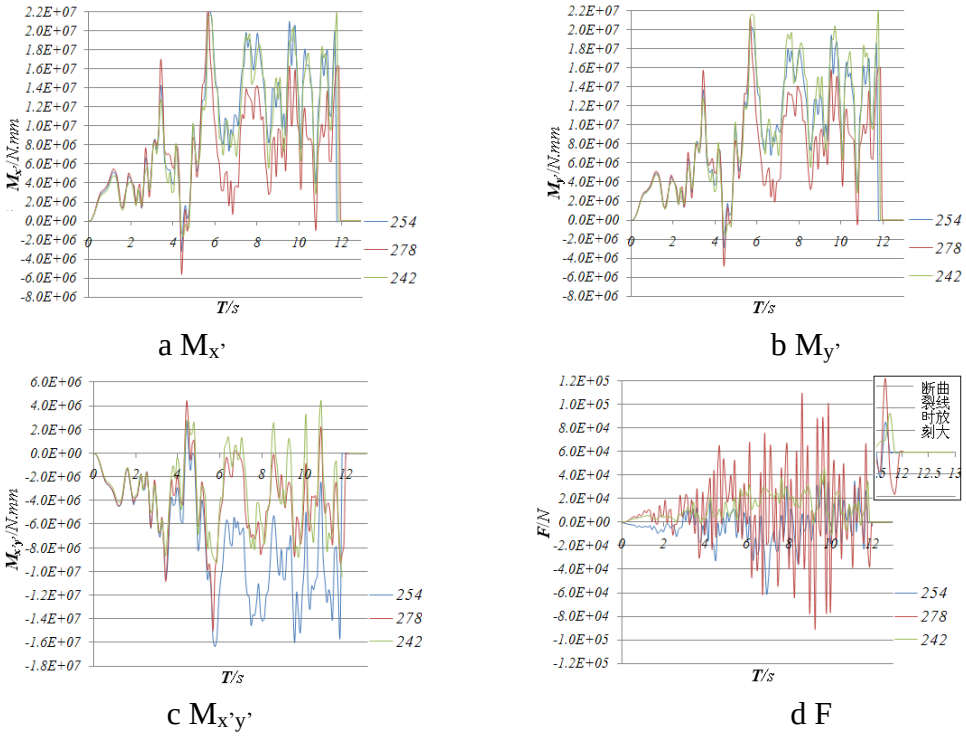

a $M_{x'}$ b $M_{y'}$

c $M_{x'y'}$ d F

Figure 9 Time history of the internal force of the diagonal members

According to Figure 10, which shows the variety of internal forces of traverse bar 14, 78 and 74 at center of zone of 2-2，traverse bar mainly is subjected to bending moment $M_{y'}$ while axial force F, bending moment $M_{x'}$, torsion $M_{x'y'}$ at this stage are minimal, so $M_{y'}$ contributed mainly to the damage increment. This is why in Fig. 11, the normal stresses of upper section fiber 3 and lower section fiber 7 were much larger than those of middle section fiber 1 and 5 which hardly exceeded yield point and casued corresponding material damage. Thus damage development concentrated in fiber 3 and 7 and traverse bars hardly failed. This is the common response observed in all the transverse bars of the monoclinic and double skew cylindrical reticulated domes under the same ground motion.

Preprints (www.preprints.org) | NOT PEER-REVIEWED | Posted: 2 May 2020 doi:10.20944/preprints202005.0012.v1

Peer-reviewed version available at Materials 2020, 13, 2519; doi:10.3390/ma13112519

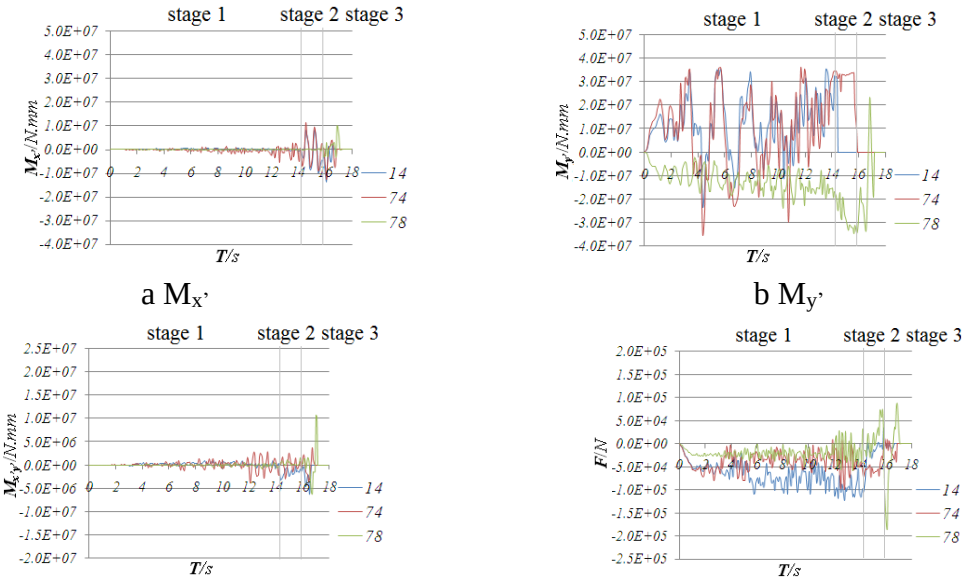

a M_x, b M_y, c $M_{x'y'}$, d F

Figure 10 time history of internal forces of traverse bar 14, 78 and 74

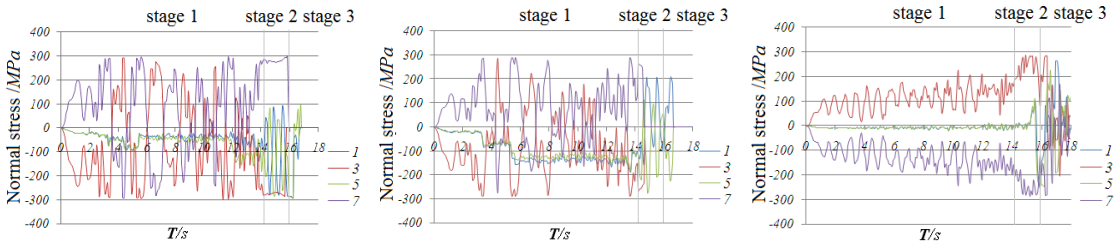

a bar 74 b bar 14 c bar 78

Figure 11 Time history of normal stress in fiber 1,3,5,7 of traverse bar 14, 78 and 74

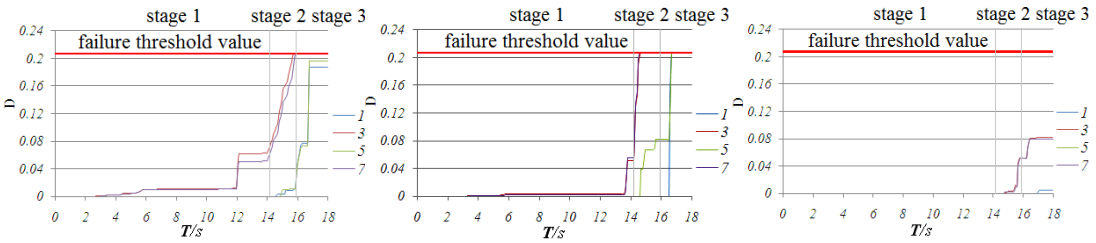

a bar 74 b bar 14 c bar 78

Figure 12 Time history of D value in fiber 1,3,5,7 of bar 14, 78 and 74

Based on the above analysis, bar 254 and neighbouring bars failed at first. And once they lose the bearing capacity, the internal-force-redistribution effect made force to be carried by the neighbouring bars that yet not failed (as it shown in Fig 11a), and D value developed rapidly untill the bar failed. Then internal-force-redistribution effect

Preprints (www.preprints.org) | NOT PEER-REVIEWED | Posted: 2 May 2020 doi:10.20944/preprints202005.0012.v1

Peer-reviewed version available at Materials 2020, 13, 2519; doi:10.3390/ma13112519

worked again. With the failure propogating, the force redistribution to the neighbouring bars continued .Finally all the bars in zone of 2-2 failed. The collapse process entered into the second stage.

Stage 2: It refers to the stage from the formation of the first "belt" in zone of 2-2 to the formation of the second "slant-bars-failed-belt" in the zone of 6-6/ 7-7（14.38s~15.83s），. In this stage, phonomen of material damage accumulation and failure of bars mainly occured during zone of 6-6 and 7-7. Effect of material damage accumulaiton cause not only the failure of all diagonal members in the zone of 2-2, but also significant deterioration of flexural stiffness of fibre 3 and 7 in the traverse bars. At this time, the dome acted as a arch whose local flexural stiffenss at zone of 2-2 weakened significantly(Fig.13).

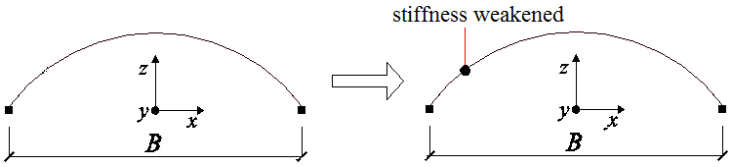

Figure 13 The transision between stage 1 and 2

In Fig. 11a, we can see that the normal stress at upper fiber 3 and lower fiber 7 at end section of traverse bar 74 was maintained at a value much greater than the yield stress of 280 MPa, while normal stress of fiber 5 and 1 also increased dramtically, which acted as a plastic hinge. Fiber 3 and 7 of traverse bar 14 failed at a short time later entering the stage, but the stress of its fiber 1 and 5 whose stress is relatively small now increased rapidly near to 200MPa. We can conclude that the normal stresses of remaining fibers of bar 14 were larger than yield point. This means that the end of bar 14 acted as a plastic hinge too. Finally we can concluded that all the traverse bars in this zone of 2-2 that yet not failed acted as plastic hinges. The formation of plastic hinges induced significant internal-force-redistribution effect. As shown in Figure 14,

Preprints (www.preprints.org) | NOT PEER-REVIEWED | Posted: 2 May 2020 doi:10.20944/preprints202005.0012.v1

Peer-reviewed version available at Materials 2020, 13, 2519; doi:10.3390/ma13112519

bending moment $M_{y'}$ axial force F, bending moment $M_{x'}$, torsion $M_{x'y'}$ of diagonal bar 161 and 232（Fig.1）, one at end and another at mid of zone of 6-6, were less than those of bar 242/254/278(Fig.8) in stage 1. So almost no damage were developped in the bars. However, the value of My' Mx', torsion Mx'y began rapid increasing since the formation of the first 'belt".

Therefore, continuously increasing internal force induced by ground motion resulted in severe damage on diagonal bars. 0.8s later entering the second stage, because the internal force of bars at two ends were larger than that of bars at mid, bars at ends in internods zone of 6-6 failed first (Fig.3g). Then other bars failed successively from two ends to middle in a short time. Finialy at 15.83s the second belt formed.

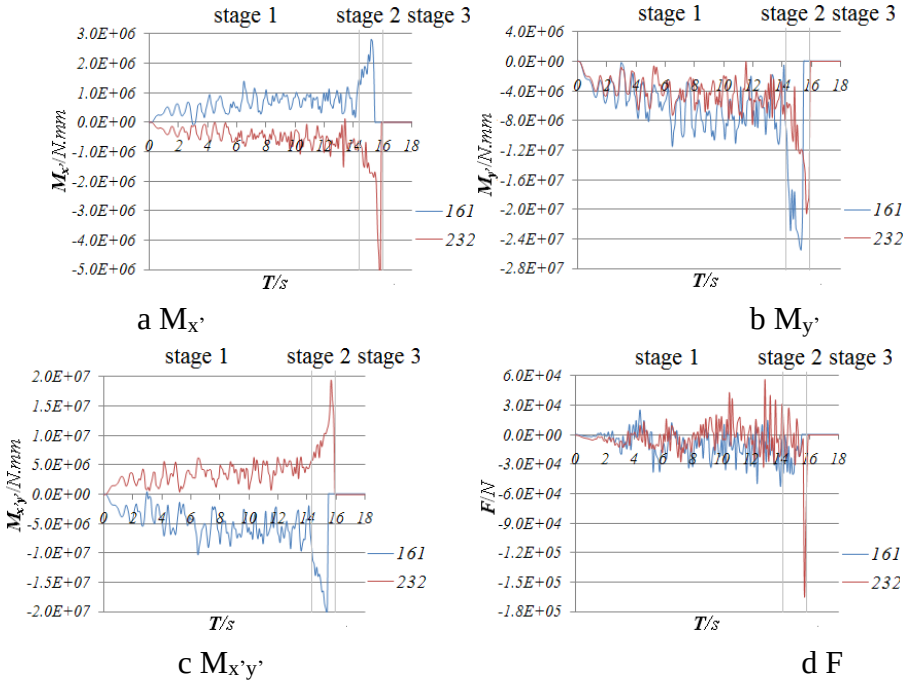

a $M_{x'}$ b $M_{y'}$

c $M_{x'y'}$ d F

Figure 14 time history of internal forces of diagonal bar 161and 232

Study on traverse bar 78, in zone of 6-6, althouge the internal forces of the bar significantly increasesd because if forece redistribution the damage accumalation mainly developped in the upper fiber 3 and lower fiber 7, while fiber 1 and 5 were not damaged seriously. So no bars failed in all fibers. In Fig.11c, the normal stresses in

Preprints (www.preprints.org) | NOT PEER-REVIEWED | Posted: 2 May 2020 doi:10.20944/preprints202005.0012.v1

Peer-reviewed version available at Materials 2020, 13, 2519; doi:10.3390/ma13112519

fiber 3 and 7 in bar 78 was very high, we could conclude that the bar acted as a plastic hinge too.

Successive failure of diagonal members and damage in traverse bars in zone of 6-6 greatly weakened the vertical stiffness of dome. So under the earthquak loading, the dome deflect downwards significantly. At the same time, angular displacement was observed at traverse bars in zone of 2-2 made damage in fiber 3 and 7 develop rapidly(Fig.11).

Untill now, the generation of the second “diagonal member failure belt” and the exist of the first “diagonal member failure belt” caused the formation of two zone whose stiffness were seriously weakened, or two plastic hinges. As showen in Fig.15, the lateral mechanism characteristics of the dome changed again.

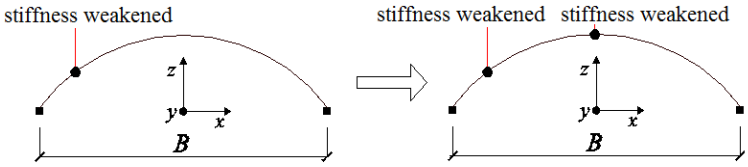

Figure 15 The transision between stage 2 and 3

Stage 3: It refers to the process transiting from the formation of the second “diagonal member failure -bar-failed belt” to final collapse of the dome (15.83s~ end) .This process is mainly a irreversible collapse process of the whole geometric configuration of dome. In two “belt”, loading is beared and transimised only by the seriously damaged traverse bars. With the development of damage and the deterioration of angle stiffness of traverse bars especially, in the vertical plane, the dome acted as a almost unstable system. Then under earthquake, the totally collapse occured, as showen in Fig.15. Calculation result showed that the process is very rapid and reversible.

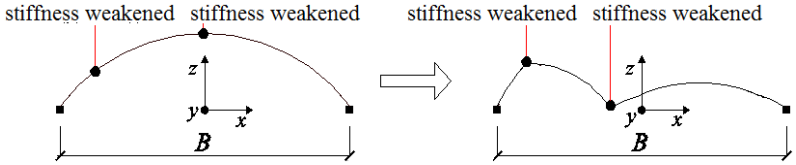

Preprints (www.preprints.org) | NOT PEER-REVIEWED | Posted: 2 May 2020 doi:10.20944/preprints202005.0012.v1

Peer-reviewed version available at Materials 2020, 13, 2519; doi:10.3390/ma13112519

Figure 16 The collapse of the dome in stage 3

Traverse bar 14 and neigbouring bars in zone of 2-2 rapidly failed because of suddenly increasing torsion. Then bending moment $M_{y'}$ of bar 74 increased obviously and made the damage value of fiber 1and 5 increase obviously.

In conclusion, in the three stages, variation of mechanical characteristics, damage zone, deformation status of dome is of distinct difference respectively. But we should understand, the three stages are closely continuous rather than intermittent or absolutely strictly divided.

3.3 Displacement during the collapse process

The deformation of the dome changed along the whole collapse process, therefore, the gravity center of the structure changed as well. Figure 17 shows the change of the locations of the center of the gravity of the structure during the whole collape process. Different peak ground acceleration was selected with the same duration of 18 s. It can be seen that the center of the gravity went down to differernt distance with differernt PGA values

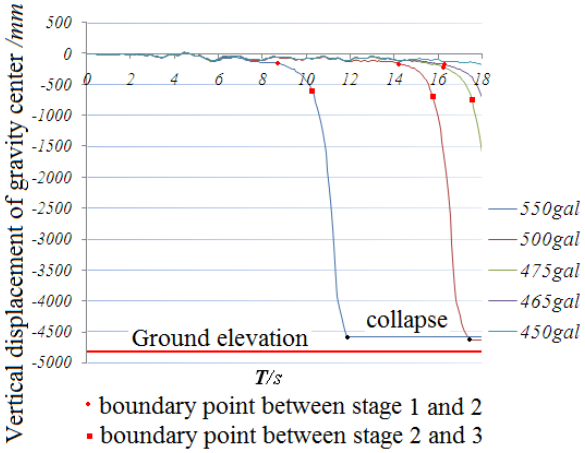

Figure 17 time history of displalcementof gravity center

When PGA is 450gal the damage was observed at 1.9 s and the rupture of the first diagonal bar occurred at 16.44s. however, the failure belt was not formed until 18 s.. at 1.9s the location of the center of the gravity fluctuated, no significant decending of the gravity center was observed.

When PGA is 465gal the first diagonal member failure belt formed at 16.55s. The second belt started to form at 17.63s. However, the failure belt was not formed until 18 s. it can also be noticed that, the slop of the curve in Figure 17 increased drantically.

When PGA is 475gal the rupture of the first diagonal member failure belt formed at 16.38s. The second belt started to form at 17.48s. However, it can also be noticed that, the slop of the curve in increased at stage 2, compare to stage 3.When PGA is 500gal the rupture of the first diagonal member failure belt formed at 14.38s. The second belt started to form at 15.83s.

It can also be seen that, when PGA is 475gal, the decending distance of the center reaches 1286mm, however, for a larger PGA 500gal, when the time is shorter than 16s, the decending distance of the center is smaller than 1286mm, which indicate the effect of the duration of the time history.

Based on above analysis, it can be concluded that:

1. At the first stage the decending of the gravity center is slow

2. The decending of the gravity center become quicker from stage 1 to stage 3

3 The time to reach stage 2 or 3 is determined by the peak ground acceleration applied to the structure, the larger the PGA, the quicker to reach stage 2 or 3.

4 The time duration will determin the collapse mechanism of the dome, which is one of the dominat factors.

4. Conclusion

In this paper, a detailed progressive collapse analysis of a single-layer cylindrical latticed shells under severe earthquakes is performed using the fibre beam element method with the inclusion of the accumulation of material damage. Below conclusion can be made:

1. A failure pattern called “double-diagonal -members-failure-belt” is discovered for this type of space structure.

2. The failure pattern can be divided into three consecutive stages:
   a. Significant variation of deformation in diiferent structural zone;
   b. Continuously increasing internal forces;
   c. Damage structural members.

Reference

[1]. American Concrete Institute (ACI). Building code requirements for structural concreteand commentary (ACI 318m-08). MI: Farmington Hills, 2008.
[2]. GSA (General Services Administration). (2003). “Progressive collapse analysis and design guidelines for new federal office buildings and major modernization projects.”
[3]. ASCE. (2010). “Minimum design loads for buildings and other structures.” SEI/ASCE 10-05, Washington, DC.
[4]. European Committee for Standardization, (2006), “Eurocode 1: Actions on structures. Part 1-7: General Actions - Accidental actions”.
[5]. European Committee for Standardization, (2004), “Eurocode 2: Design of concrete structures. Part 1-1: General rules and rules for buildings”.
[6]. FEMA (Federal Emergency Management Agency). (2002). “World trade center building performance study: Data collection, preliminary observations, and recommendations.” FEMA 403, Washington, DC.
[7]. NIST (National Institute of Science and Technology). (2005). “Final report on the collapse of the world trade center towers.” NCSTAR 1, U.S. Dept. of Commerce, Gaithersburg, MD.
[8]. McGuire, W., (1974). “Prevention of progressive collapse.” Proc., Regional Conf. on Tall Buildings, Asian Institute of Technology, Bangkok.
[9]. Shimada, Y., Matsuoka, Y., Yamada, S., and Suita, K. (2008). “Dynamic collapse test on 3-D steel frame model.” The 14th World Conf. on Earthquake Engineering, Beijing.
[10]. Song BI , Giriunas KA , Sezen H ,(2014). “Progressive collapse testing and analysis of a steel frame building”. J. Constr. Steel Res., 94(3), 76-83.
[11]. Chen, J.L., Peng, W.B., Huang, X., (2012). “Experimental study on progressive collapse resistance of two-storey steel moment-frame with composite slabs”. J. Tongji University. 40(9), 1300-1305
[12]. Tsitos, A., Mosqueda, G., Filiatrault, A., Reinhorn, A.M.(2010). “Experimental investigation of the progressive collapse of a steel post-tensioned energy dissipating frame”. 10th Canadian Conference on Earthquake Engineering

[13]. Starossek (2006). “Progressive collapse of structures: Nomenclature and procedures”. Struct. Eng. Int., 16(2), 113–117.
[14]. Lim, J., Krauthammer, T., (2006). “Progressive collapse analyses of 2D steel-framed structures with different connection models”. Eng. J., 43(3), 201-215
[15]. Yamazaki, S., Minami, S., (2010). “Progressive collapse of multi-story steel frames”. J. Struc. and Constr. Eng.,75(648), 415-423
[16]. O'Dwyer, D., Janssens, V., (2010) , “Modelling progressive collapse of structures”, Civil-Comp Proceedings, 10th International Conference on Computational structures technology, 93.
[17]. Zheng, H.D., Fan, J., (2018). “Analysis of the progressive collapse of space truss structures during earthquakes based on a physical theory hysteretic model”. Thin-Walled Struct., 23, 70-81.
[18]. Rashidyan, S., Sheidaii, M., (2017), “Improving double-layer space trusses collapse behavior by strengthening compression layer and weakening tension layer members”. Advances in Struct. Eng., 20(11),1757-1767.
[19]. Lau, D.T. , Wibowo, H.,(2010), “Seismic progressive collapse analysis of reinforced concrete bridges by applied element method”, Proceedings of the 12th Int. Con. on Eng., Science, Constr., and Operations in Challenging Environments - Earth and Space,3019-3026.
[20]. Miyachi, K., Nakamura, S., Manda, A.,(2012), “Progressive collapse analysis of steel truss bridges and evaluation of ductility”, J. of Constructional Steel Research,78(6), 192-200
[21]. Takeuchi, T., Horiuchi, K., Matsui, R., Ogawa, T., Imamura, A., (2014), “Collapse mechanism of truss tower structures including buckling and fracture of tubular members”, J. Struct. and Constr. Eng. 79(703), 1309-1319
[22]. Ponter, A., Chen, H.F., (2001), “A programming method for limit load and shakedown analysis of structures”, Pressure Vessels and Piping Division (Publication) PVP, 430, 155-162.
[23]. Skordeli MAA, Bisbos CD (2010), “Limit and shakedown analysis of 3D steel frames via approximate ellipsoidal yield surfaces”, Eng. Struct., 32 (6),1556-1567
[24]. Ferrari, R., Cocchetti, G., Rizzi, E.,(2018), “Computational elastoplastic Limit Analysis of the Paderno d'Adda bridge (Italy, 1889)”, Archives of Civil and Mechanical Eng., 18(1), 291-310.
[25]. Xia, K.Q., Yao, W.X., Dong, S.L., (2002), “Dynamic behavior of snap-through buckling in reticulated domes”, Eng. Mechanics, 19(1), 9-13Blandford, G.E.,(1996), “Large deformation analysis of inelastic space truss structures”, J. Struct. Eng. N.Y., 122(4), 407-415
[26]. Kato, S., Mutoh, I., Shomura, M. (1998). “Collapse of semi-rigidly jointed reticulated domes with initial geometric imperfections.” J. Constr. Steel Res., 48(2–3), 145–168
[27]. Zhou, H., Zhang, Y.G., Fu, F. and Wu, J.Z. (2018) “Progressive Collapse Analysis of Reticulated Shell under Severe Earthquake considering the Damage Accumulation Effect.” Journal of Performance of Constructed Facilities, April 2018 Volume 32, Issue 2.